

Magnetic correlations and superconducting pairing near higher-order Van Hove singularities

Zheng Wei,¹ Yanmei Cai,¹ Boyang Wen,¹ and Tianxing Ma^{1,2,*}

¹*School of Physics and Astronomy, Beijing Normal University, Beijing 100875, China*

²*Key Laboratory of Multiscale Spin Physics (Ministry of Education),
Beijing Normal University, Beijing 100875, China*

(Dated: Version 16.0 – May 16, 2025)

We explore magnetic correlations and superconducting pairing near higher-order Van Hove singularities in an extended Hubbard model on honeycomb lattice incorporating third-nearest-neighbor hopping t'' . Using quantum Monte Carlo methods, we identify a crossover between ferromagnetic and antiferromagnetic fluctuations near higher-order Van Hove singularities filling, where t'' enhances ferromagnetic correlations below while suppressing antiferromagnetic fluctuations toward half-filling. At low doping, f_n -wave pairing dominates, amplified by higher-order Van Hove singularities-induced divergent density of states. Remarkably, despite general suppression of f_n -wave pairing by increasing next-nearest neighbor hopping t' and t'' , a critical $t'' = 0.15$ triggers anomalous enhancement via higher-order Van Hove singularities renormalization at a fix t' . The nearest-neighbor Coulomb interactions V suppress superconducting correlation, which exhibiting sign-independent suppression proportional to $|V|$. These results highlight the interplay of higher-order Van Hove singularities-driven electronic structure, magnetic fluctuations, and pairing symmetry competition in electron correlated systems.

INTRODUCTION

In the realm of strongly correlated electron systems, the exploration of unconventional superconductivity stands as one of the most captivating frontiers in condensed matter physics[1]. Unlike conventional superconductors, where phonon-mediated pairing gives rise to Bardeen-Cooper-Schrieffer (BCS) superconductivity, unconventional superconductors typically emerge from intricate electronic interactions, yielding exotic pairing symmetries and non-trivial order parameters[1, 2]. Extensive investigations have demonstrated that magnetic fluctuations driven by strong electron correlations play a pivotal role in mediating Cooper pairing, as seen in doped cuprates[3], iron-based superconductors[4], and heavy-fermion systems[5]. Specifically, triplet pairing may arise from ferromagnetic-like spin fluctuations, while singlet pairing with d -wave symmetry is often associated with antiferromagnetic spin fluctuations[1, 6]. This dichotomy undergoes the ongoing debate about the competition between different superconducting pairing symmetries and magnetic modes.

The influence of electronic correlations on superconductivity can be significantly amplified in systems with singular features in their electronic density of states (DOS). Materials hosting van Hove singularities (VHS) have drawn substantial attention due to the interplay between magnetism and superconductivity, where VHS-enhanced structural and magnetic instabilities may compete with superconducting states[7–11]. A striking example is the magic-angle graphene superlattice system, in which scientists observed unconventional superconductivity closely tied

to strong electron correlation effects[12–14]. This correlation is further amplified by the extreme DOS induced by VHS, offering critical insights into the understanding of unconventional superconductivity[15].

In recent years, an especially intriguing scenario has emerged in materials with higher-order van Hove singularities (HOVH), where the electronic DOS diverges in a power-law manner due to the presence of saddle points with higher-order band flattening[7, 16–19]. Unlike conventional van Hove singularities, which exhibit a logarithmic DOS divergence. HOVH systems can sustain markedly enhanced electronic correlations, amplifying the effects of interactions such as spin fluctuations, charge instabilities, and unconventional superconductivity[20, 21].

Theoretical and experimental evidence is emerging to suggest that strong electron-electron interactions induced by HOVH may give rise to a distinct type of chiral superconductivity, characterized by a unique pairing symmetry that deviates from conventional superconducting mechanisms[22]. These singularities have also been shown to trigger quantum phase transitions, leading to substantial modifications in the topological properties of materials and even the emergence of topological superconductivity[14, 23]. The HOVH not only enhances the electronic anisotropy of materials, instigating a competition between ferromagnetic (FM) and antiferromagnetic (AFM) fluctuations[7], but also promotes Stoner-type magnetism due to the extreme DOS. Moreover, it provides a favorable environment for long-range electron pairing, potentially stabilizing superconducting phases beyond the standard BCS paradigm[1].

Inspired by the intriguing correlated phenomena

discovered in graphene-based systems, the Hubbard model on a honeycomb lattice has become a paradigmatic theoretical framework for exploring strong electron correlations in quantum materials. Beyond its Dirac physics at half filling, this prototypical system exhibits VHS in its low-energy spectrum, with the saddle points of the band structure leading to a divergent DOS[24]. Notably, when these saddle points acquire higher-order characteristics (e.g., through strain, twisting, or doping), the singularities evolve into higher-order Van Hove singularities, leading to a more dramatic amplification of the DOS. In such regimes, the enhanced electronic correlations near HOVH create a fertile platform for intertwined orders, including unconventional superconductivity and complex magnetic phases[25].

The Hubbard model on a honeycomb lattice has been intensively studied for decades. At half-filling, quantum Monte Carlo (QMC) studies indicate that when the on-site Coulomb repulsion energy U exceeds the critical value $U_c \approx 3.8t$, where t is the nearest-neighbor (NN) hopping, the system undergoes a transition from a semimetal to a Mott insulator, accompanied by the emergence of AFM long-range order[26–28]. When the system is away from half-filling, electron correlations may induce unconventional superconductivity: near half-filling, superconducting pairing is often dominated by the $d + id$ wave (chiral d wave)[25, 29–37], which originates from the mediation of AFM spin fluctuations. In the large-doping region ($\langle n \rangle \simeq 0.2$), when the Fermi level is close to the HOVH singularity at the bottom of the energy band induced by the next-nearest-neighbor (NNN) hopping term t' , the $p + ip$ wave (chiral p wave) triplet pairing becomes dominant[6, 38–40]. This dominant superconducting pairing is driven by FM fluctuations, and the power-law divergence of the DOS near the HOVH may significantly increase the superconducting critical temperature. However, although the role of HOVH in enhancing electron correlations and superconducting pairing has been preliminarily explored, the reported filling region is rather low, making experimental detection nearly impossible[6].

In honeycomb lattices, the complex interplay between HOVH singularities and correlation-driven instabilities—such as superconductivity and magnetic order—remains a profound mystery. This work expands the existing framework by incorporating the third-nearest-neighbor (TNN) hopping parameter t'' : using the determinant quantum Monte Carlo (DQMC) method, we investigate the impact of t'' on magnetic correlations and observe a crossover between FM and AFM fluctuations at different electron fillings. By employing constrained-path Monte Carlo method, we focus on electron correlation-driven superconducting pairing near HOVH under various conditions of electron filling $\langle n \rangle$, hopping parameters t' and t'' , and nearest-

neighbor Coulomb interaction V . Our findings reveal that near the HOVH filling, superconducting pairing with f_n -symmetry becomes dominant, and this pairing may be driven by competing FM/AFM fluctuations.

MODEL AND METHODS

The system we simulated is sketched in Fig.1 (a), and the honeycomb lattice structure consists of two sublattices: the A sublattice, represented by blue circles, and the B sublattice, denoted by red circles. The first Brillouin zone (BZ), depicted in Fig. 1(b), shows high-symmetry points along standard paths, essential for electronic structure analysis.

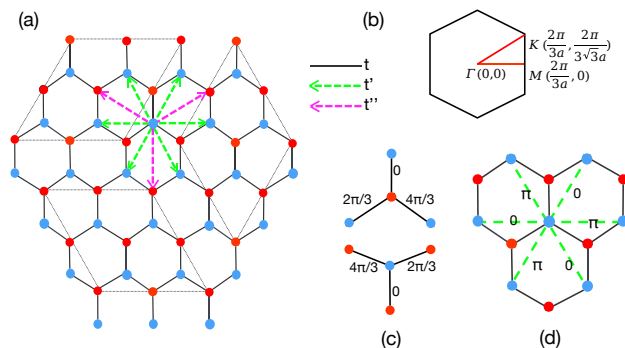


FIG. 1. (a) Sketch of honeycomb lattice with double-27 sites of $N = 2 \times 3L^2$ with $L = 3$; (b) the first Brillouin zone and high symmetry points; (c) the form of NN $d + id$ pairing symmetry; (d) the form of NNN f_n pairing symmetry.

We began by constructing a theoretical model for the honeycomb lattice based on the Hubbard model:

$$\begin{aligned}
 H &= H_k + H_U - \mu \sum_{i\sigma} n_{i\sigma} \\
 H_k &= -t \sum_{\langle i,j \rangle \sigma} c_{i\sigma}^\dagger c_{j\sigma} - t' \sum_{\langle\langle i,j \rangle\rangle \sigma} c_{i\sigma}^\dagger c_{j\sigma} \\
 &\quad - t'' \sum_{\langle\langle\langle i,j \rangle\rangle\rangle \sigma} c_{i\sigma}^\dagger c_{j\sigma} + \text{H.c.} \\
 H_U &= U \sum_i n_{i\uparrow} n_{i\downarrow} + V \sum_{\langle i,j \rangle \sigma \sigma'} n_{i\sigma} n_{j\sigma'} \quad (1)
 \end{aligned}$$

Here, t , t' , and t'' denote the hopping integrals between nearest-neighbor, next-nearest-neighbor, and third-nearest-neighbor sites, respectively. The indices i and j signify lattice sites. The operators $c_{i\sigma}^\dagger$ and $c_{j\sigma}$ are used to create and annihilate an electron with spin σ at sites i and j , respectively. The operator $n_{i\sigma} = c_{i\sigma}^\dagger c_{i\sigma}$ quantifies the number of electrons with spin σ at site i . U represents the on-site Coulomb interaction strength, while V stands for the NN Coulomb interaction

strength. The chemical potential μ is utilized to regulate the electron concentration.

Compared to the pristine honeycomb lattice with only NN hopping t , the inclusion of long-range hoppings t' and t'' enhances electron delocalization while intensifying geometric frustration. This dual effect modifies the electronic band structure and shifts the HOVH singularity position. To quantitatively determine the HOVH location, we analyze the non-interacting ($U = 0$) band dispersion:

$$E_{\pm}(\vec{k}) = \pm |t\alpha(\vec{k}) + t''\gamma(\vec{k})| - t'\beta(\vec{k})$$

Here $\alpha(\vec{k}) = \sum_{i=1}^3 e^{-i\vec{k}\cdot\vec{a}_i}$, $\beta(\vec{k}) = \sum_{i=1}^6 e^{-i\vec{k}\cdot\vec{b}_i}$, $\gamma(\vec{k}) = \sum_{i=1}^3 e^{-i\vec{k}\cdot\vec{c}_i}$, with \vec{a}_i , \vec{b}_i , and \vec{c}_i denote NN, NNN, and TNN displacement vectors, respectively. Expanding $E(\vec{k})$ around the M -point up to quadratic order, we identify the HOVH condition when the effective mass tensor becomes singular. Specifically, the critical relation[41]

$$t'' = \frac{t - 2t'}{4} \quad (2)$$

signals a topological transition at the saddle point, where the conventional VHS evolves into a HOVH through Berry curvature restructuring. This transition is reflected in the change from the black solid line to the red solid line, as demonstrated in Fig. 2.

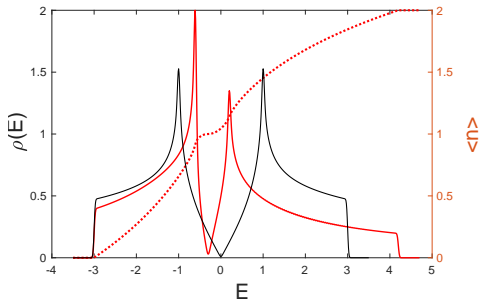


FIG. 2. The DOS as functions of energy with $t = 1.00$, $t' = 0$ (black solid line) and $t = 1.00$, $t' = 0.10$, $t'' = 0.20$ (red solid line). And the red dotted line shows fillings (n) as a function of energy with $t = 1.00$, $t' = 0.10$, and $t'' = 0.20$

In our simulations, we employed a two dimensional honeycomb lattice with periodic boundary conditions. The system size was set to $L = 4$ and 5 , leading to a total of $N = 2 \times 3L^2$ lattice sites. This parameter selection enables us to investigate fundamental physical phenomena within a computationally tractable framework while effectively capturing the essential characteristics of the honeycomb lattice structure. The system is studied using complementary

quantum Monte Carlo approaches: DQMC for finite-temperature properties[42–45] and CPMC for ground-state characterization[29, 33, 46–49]. The DQMC methodology employs a stochastic evaluation of the partition function through auxiliary field discretization, where the high-dimensional integration is performed via importance sampling with controlled Trotter errors. In contrast, the CPMC approach projects the ground-state wavefunction through imaginary-time evolution within a constrained manifold of Slater determinants, enforced by a trial wavefunction $|\psi_T\rangle$ that maintains positive overlaps throughout the random walk process. Extensive benchmarking confirms the constraint-induced systematic error remains below 3% for measured observables, with ground-state properties showing remarkable insensitivity to the specific choice of $|\psi_T\rangle$ [42]. Our implementation utilizes closed-shell filling configurations and adopts a free-electron trial wavefunction, $|\psi_T\rangle = \prod_{k \leq k_F} c_k^\dagger |0\rangle$, where the Fermi surface corresponds to the non-interacting system. This construction ensures computational efficiency while preserving physical consistency with the metallic phase under investigation, achieving an optimal balance between numerical tractability and systematic error control.

To study magnetic fluctuations, we defined the spin susceptibility in the z -direction at zero frequency as follows:

$$\chi_s(\mathbf{q}) = \frac{1}{N} \int_0^\beta d\tau \sum_{i,j} e^{i\mathbf{q}\cdot(\mathbf{r}_i - \mathbf{r}_j)} \langle S_i^z(\tau) S_j^z(0) \rangle \quad (3)$$

Here, $\chi_s(\Gamma)$ quantifies ferromagnetic correlations, and $\chi_s(M)$ quantifies antiferromagnetic correlations.

Within the CPMC framework, we investigate long-range superconducting pairing correlations by analyzing pairing correlation functions for various pairing symmetries. The pairing correlation function is defined as:

$$C_\alpha(r) = \frac{1}{N} \sum_i \langle \Delta_\alpha^\dagger(\mathbf{r}_i + \mathbf{r}) \Delta_\alpha(\mathbf{r}_i) \rangle \quad (4)$$

For the NN pairing (e.g., $d + id$ pairing), the pairing operator takes the form[50, 51]:

$$\Delta_{d+id}(\mathbf{r}_i) = \sum_\delta \eta_{d+id}(\delta) (c_{i\uparrow} c_{i+\delta\downarrow} - c_{i\downarrow} c_{i+\delta\uparrow}) \quad (5)$$

For the NNN pairing (e.g., f_n pairing), the pairing operator is given by:

$$\Delta_{f_n}(\mathbf{r}_i) = \sum_{\delta'} \eta_{f_n}(\delta') (c_{i\uparrow} c_{i+\delta'\downarrow} + c_{i\downarrow} c_{i+\delta'\uparrow}) \quad (6)$$

The form factors for NN $d + id$ pairing and NNN f_n

pairing are given as follows:

$$\eta_{d+id}(\delta) = \begin{cases} 1, & \delta = \vec{a}_1 \\ e^{i2\pi/3}, & \delta = \vec{a}_2 \\ e^{i4\pi/3}, & \delta = \vec{a}_3 \end{cases} \quad (7)$$

$$\eta_{f_n}(\delta') = \sin\left(\frac{\mathbf{k} \cdot \delta'}{2}\right), \quad \delta' = \vec{a}_1, \vec{a}_2, \dots, \vec{a}_6 \quad (8)$$

Their pairing symmetry configurations are sketched in Fig.1(c) and Fig.1 (d), respectively.

RESULTS AND DISCUSSION

We begin by setting the hopping parameters $t = 1.00$, $t' = 0.10$, and Hubbard interaction $U = 3.0|t|$, while varying TNN hopping t'' across different electron fillings $\langle n \rangle = 0.50, 0.75, 0.81$, and 1.00 . Our study focus on the influence of t'' on spin susceptibility. The results demonstrate distinct behaviors in spin susceptibility between two filling regions separated by the HOVH singularity. Notably, a crossover from FM to AFM correlations emerges at $\langle n \rangle = 0.75$, as shown in Fig. 3.

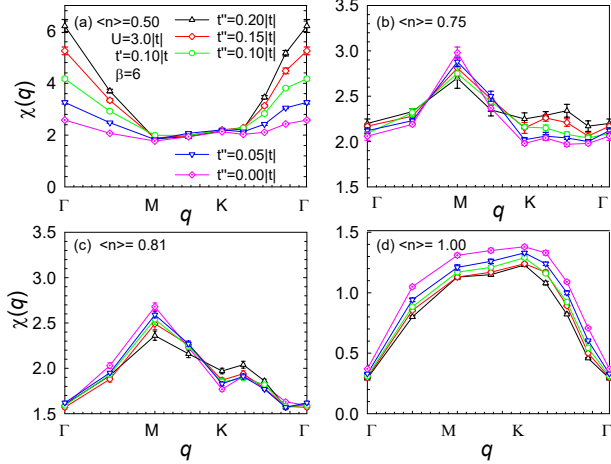


FIG. 3. The relationship between the spin susceptibility and \mathbf{q} for different TNN hopping integrals t'' at fixed $U = 3.0|t|$ and $\beta = 6$. (a) $\langle n \rangle = 0.50$; (b) $\langle n \rangle = 0.75$; (c) $\langle n \rangle = 0.81$; (d) $\langle n \rangle = 1.00$.

Specifically, in the filling region below the HOVH singularity (i.e., $\langle n \rangle = 0.50$), the system predominantly exhibits FM behavior, which is significantly enhanced with increasing t'' . Near the HOVH filling at $\langle n \rangle = 0.75$, FM and AFM correlations compete: t'' suppresses FM fluctuations at the M-point while enhancing it at the Γ -points. In contrast, within the filling range from HOVH to half-filling ($\langle n \rangle = 1.00$), the system primarily displays AFM correlations that are suppressed by increasing

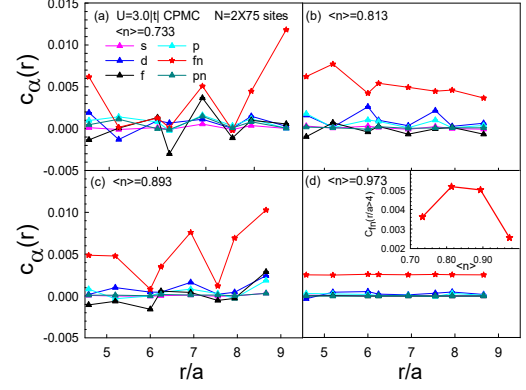


FIG. 4. The pairing correlation as a function of distance for different pairing symmetries with (a) $\langle n \rangle = 0.733$; (b) $\langle n \rangle = 0.813$; (c) $\langle n \rangle = 0.893$; (d) $\langle n \rangle = 0.973$.

t'' . These results provide further support for previous findings.

To explore the property of superconducting pairing, we set the hopping parameters to $t = 1.00$, $t' = 0.10$, and $t'' = 0.20$, and identify the filling $\langle n \rangle = 0.881$ as corresponding to the HOVH singularity. For an on-site Coulomb interaction $U = 3.0|t|$, we focus on closed-shell fillings near $\langle n \rangle = 0.881$.

The results presented in Fig. 4 reveal that the f_n -wave pairing symmetry dominates over other symmetries, followed by the $d + id$ -wave. As the electron filling $\langle n \rangle$ decreases from 0.973 to 0.813, the average f_n -wave pairing correlation is significantly enhanced. In contrast, when $\langle n \rangle$ deviates further from 0.813, the f_n -wave correlations are suppressed. This underscores the pivotal role of the HOVH singularity in enhancing pairing correlations.

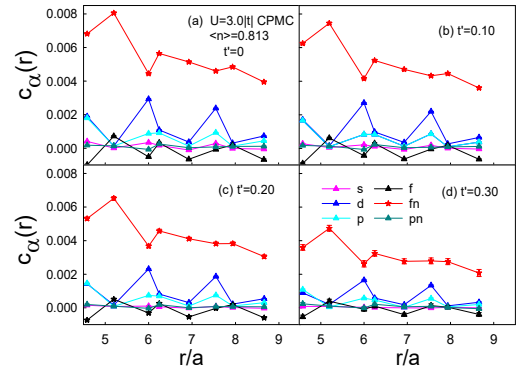


FIG. 5. Pairing correlation functions for different pairing symmetries with (a) $t' = 0$; (b) $t' = 0.10$; (c) $t' = 0.20$; (d) $t' = 0.30$.

To investigate the influence of the NNN hopping t' on long-range superconducting pairing correlations, we

fix the electron filling to $\langle n \rangle = 0.813$, with hopping parameters $t = 1.00$ and $t'' = 0.15$, while systematically varying t' from 0 to 0.30. As shown in Fig. 5, both the f_n -wave and $d+id$ -wave pairing correlation functions exhibit a monotonic suppression as t' increases.

A similar analysis of the effect of t'' on pairing correlations is performed with $\langle n \rangle = 0.813$, $t = 1.00$, and $t' = 0.20$, while t'' ranges from 0 to 0.30 in Fig. 6. Here, the f_n -wave remains dominant, and at $t'' = 0.15$, the superconducting pairing correlations exhibit an unexpected strengthening due to the HOVH effect.

The observed transition from FM to AFM correlations across the HOVH singularity, coupled with the dominant f_n -wave superconducting pairing near $\langle n \rangle = 0.813$, reveals a profound interplay between magnetic fluctuations and unconventional superconductivity. Below the HOVH filling ($\langle n \rangle < 0.75$), the enhanced FM correlations with increasing t'' suggest a Stoner-type instability that typically competes with spin-singlet pairing. However, the emergence of robust f_n -wave superconductivity near $\langle n \rangle = 0.813$, precisely where FM and AFM correlations compete, implies a complex mediation mechanism: while strong FM fluctuations would normally suppress conventional superconductivity, the proximity to the HOVH singularity may enable an unconventional pairing channel through the unique momentum-space structure of spin fluctuations near the HOVH point. These results collectively suggest that the HOVH singularity not only enhances pairing correlations through its singular density of states but also creates a unique magnetic environment where competing FM/AFM fluctuations may actively mediate unconventional superconductivity.

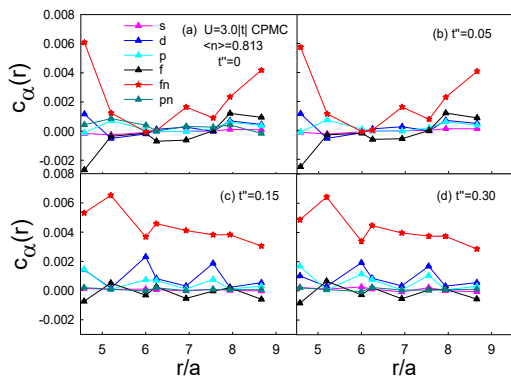


FIG. 6. Pairing correlation functions for different pairing symmetries with (a) $t'' = 0$; (b) $t'' = 0.05$; (c) $t'' = 0.15$; (d) $t'' = 0.30$.

The influence of t'' on both FM and AFM correlations, alongside the non-monotonic enhancement of f_n -wave pairing at $t'' = 0.15$, further suggests that TNN hopping tunes the system through a sweet spot where the HOVH-enhanced DOS cooperates with residual magnetic

fluctuations to stabilize f_n -wave pairing. This behavior bears resemblance to the spin-fluctuation-mediated pairing scenarios, where competition between different magnetic modes can promote unconventional pairing symmetries. The dominance of f_n -wave pairing may be particularly favored by the anisotropic spin fluctuations emerging near the HOVH filling, as evidenced by the t'' -dependent modulation of susceptibility at Γ , K , and M points.

Finally, we delve into the specific impact of V on f_n -wave pairing correlations in Fig. 7. Increasing V suppresses f_n -wave pairing correlations, regardless of its sign, which is similar in many other systems.

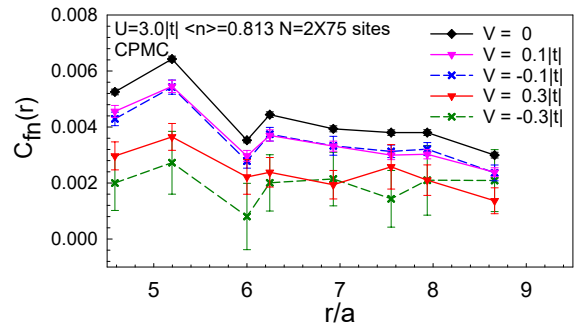


FIG. 7. Behavior of pairing correlation functions for f_n -wave symmetry under varying NN interaction strengths V .

CONCLUSION

In this work, we have systematically investigated the magnetic correlations and superconducting pairing near HOVH singularities by employing DQMC and CPMC methods. We observed a crossover from FM to AFM correlations in the vicinity of the HOVH filling, driven by the interplay between TNN hopping t'' and electronic DOS divergence. Below the HOVH, t'' amplifies FM fluctuations, while suppressing AFM correlations at higher fillings approaching half-filling. In the filling regime $\langle n \rangle \sim 0.8$, f_n -wave pairing symmetry dominates, with HOVH-induced power-law divergence in the DOS significantly enhancing superconducting correlations. Interestingly, while larger t' and t'' values generally suppress f_n -wave pairing, a critical $t'' = 0.15$ triggers an anomalous enhancement of pairing correlations at a fixed t' due to the HOVH effect. These results not only advance our understanding of the competitive mechanisms between magnetic fluctuations and unconventional superconductivity in HOVH systems but also provide a theoretical respect for tailoring correlated electronic phases in graphene-derived quantum materials through strain, doping, or interaction engineering.

This work was supported by NSFC (12474218 and 12088101) and Beijing Natural Science Foundation (No. 1242022 and 1252022). The numerical simulations in this work were performed at the HSCC of Beijing Normal University.

* txma@bnu.edu.cn

- [1] D. J. Scalapino, *Rev. Mod. Phys.* **84**, 1383 (2012).
- [2] D. Podolsky and E. Demler, *Interplay of magnetism and superconductivity in strongly correlated electron systems*, Ph.d., Harvard University, United States – Massachusetts (2005).
- [3] J. G. Bednorz and K. A. Müller, *Zeitschrift für Physik B Condensed Matter* **64**, 189 (1986).
- [4] Y. Kamihara, T. Watanabe, M. Hirano, and H. Hosono, *Journal of the American Chemical Society* **130**, 3296 (2008).
- [5] F. Steglich, J. Aarts, C. D. Bredl, W. Lieke, D. Meschede, W. Franz, and H. Schäfer, *Phys. Rev. Lett.* **43**, 1892 (1979).
- [6] T. Ma, F. Yang, H. Yao, and H.-Q. Lin, *Phys. Rev. B* **90**, 245114 (2014).
- [7] X. Han, A. P. Schnyder, and X. Wu, *Phys. Rev. B* **107**, 184504 (2023).
- [8] E. Wang, L. Pullasser, and L. H. Santos, *Phys. Rev. B* **111**, 075114 (2025).
- [9] Y.-C. Lee, D. V. Chichinadze, and A. V. Chubukov, *Phys. Rev. B* **109**, 155118 (2024).
- [10] P. Castro, D. Shaffer, Y.-M. Wu, and L. H. Santos, *Phys. Rev. Lett.* **131**, 026601 (2023).
- [11] P. A. Igoshev and A. A. Katanin, *Phys. Rev. B* **107**, 115105 (2023).
- [12] Y. Cao, V. Fatemi, S. Fang, K. Watanabe, T. Taniguchi, E. Kaxiras, and P. Jarilloherrero, *Nature* **556**, 43 (2018).
- [13] A. S. Shankar, D. O. Oriekhov, A. K. Mitchell, and L. Fritz, *Phys. Rev. B* **107**, 245102 (2023).
- [14] D. Guerci, P. Simon, and C. Mora, *Phys. Rev. Res.* **4**, L012013 (2022).
- [15] Y. Cao, V. Fatemi, A. Demir, S. Fang, S. L. Tomarken, J. Y. Luo, J. D. Sanchez-Yamagishi, K. Watanabe, T. Taniguchi, E. Kaxiras, R. C. Ashoori, and P. Jarillo-Herrero, *Nature* **556**, 80 (2018).
- [16] N. F. Q. Yuan, H. Isobe, and L. Fu, *Nature Communications* **10**, 5769 (2019).
- [17] Y. Hu, X. Wu, B. R. Ortiz, S. Ju, X. Han, J. Ma, N. C. Plumb, M. Radovic, R. Thomale, S. D. Wilson, A. P. Schnyder, and M. Shi, *Nature Communications* **13**, 2220 (2022).
- [18] H. Tan, Y. Jiang, G. T. McCandless, J. Y. Chan, and B. Yan, *Phys. Rev. Res.* **6**, 043132 (2024).
- [19] A. Zervou, D. V. Efremov, and J. J. Betouras, *Phys. Rev. Res.* **5**, L042006 (2023).
- [20] C. Wu, D. Bergman, L. Balents, and S. Das Sarma, *Phys. Rev. Lett.* **99**, 070401 (2007).
- [21] M. M. Scherer, S. Uebelacker, and C. Honerkamp, *Phys. Rev. B* **85**, 235408 (2012).
- [22] R. Nandkishore, L. S. Levitov, and A. V. Chubukov, *Nature Physics* **8**, 158 (2012).
- [23] X. Han, J. Zhan, F.-C. Zhang, J. Hu, and X. Wu, *Science Bulletin* **69**, 319 (2024).
- [24] T. Ma, F. Hu, Z. Huang, and H.-Q. Lin, *Applied Physics Letters* **97**, 112504 (2010).
- [25] P. Jia, S. Yang, W. Li, J. Yang, T. Ying, X. Li, and X. Sun, *Physics Letters A* **442**, 128175 (2022).
- [26] T. Ma, L. Zhang, C.-C. Chang, H.-H. Hung, and R. T. Scalettar, *Phys. Rev. Lett.* **120**, 116601 (2018).
- [27] S. Sorella, Y. Otsuka, and S. Yunoki, *Scientific Reports* **2**, 992 (2012).
- [28] F. F. Assaad and I. F. Herbut, *Phys. Rev. X* **3**, 031010 (2013).
- [29] T. Ma, Z. Huang, F. Hu, and H.-Q. Lin, *Phys. Rev. B* **84**, 121410 (2011).
- [30] S.-C. Fang, X.-J. Zheng, H.-Q. Lin, and Z.-B. Huang, *Journal of Physics: Condensed Matter* **33**, 025601 (2020).
- [31] S.-C. Fang, G.-K. Liu, H.-Q. Lin, and Z.-B. Huang, *Phys. Rev. B* **100**, 115135 (2019).
- [32] H. Dai, J. Hou, X. Zhang, Y. Liang, and T. Ma, *Phys. Rev. B* **104**, 035104 (2021).
- [33] H. Dai, R. Ma, X. Zhang, T. Guo, and T. Ma, *Phys. Rev. B* **107**, 245106 (2023).
- [34] K. Guo, Y. Zhang, Y. Liang, and T. Ma, *Phys. Rev. B* **110**, 085103 (2024).
- [35] S. Yang and T. Ying, *Frontiers of Physics* **18**, 33305 (2022).
- [36] X.-D. Li, H.-R. Liu, Z.-D. Yu, C.-D. Gong, S.-L. Yu, and Y. Zhou, *New Journal of Physics* **24**, 103035 (2022).
- [37] X. Y. Xu, S. Wessel, and Z. Y. Meng, *Phys. Rev. B* **94**, 115105 (2016).
- [38] T. Ying and S. Yang, *Phys. Rev. B* **102**, 125125 (2020).
- [39] H. Yao and F. Yang, *Phys. Rev. B* **92**, 035132 (2015).
- [40] X. Chen, Y. Yao, H. Yao, F. Yang, and J. Ni, *Phys. Rev. B* **92**, 174503 (2015).
- [41] L. Classen, A. V. Chubukov, C. Honerkamp, and M. M. Scherer, *Phys. Rev. B* **102**, 125141 (2020).
- [42] S. Sorella, G. B. Martins, F. Becca, C. Gazza, L. Capriotti, A. Parola, and E. Dagotto, *Phys. Rev. Lett.* **88**, 117002 (2002).
- [43] R. Blankenbecler, D. J. Scalapino, and R. L. Sugar, *Phys. Rev. D* **24**, 2278 (1981).
- [44] S.-Q. Su, Z.-B. Huang, and H.-Q. Lin, *Journal of Applied Physics* **103**, 07C717 (2008).
- [45] R. T. Scalettar, E. Y. Loh, J. E. Gubernatis, A. Moreo, S. R. White, D. J. Scalapino, R. L. Sugar, and E. Dagotto, *Phys. Rev. Lett.* **62**, 1407 (1989).
- [46] H. Nguyen, H. Shi, J. Xu, and S. Zhang, *Computer Physics Communications* **185**, 3344 (2014).
- [47] S. Zhang, J. Carlson, and J. E. Gubernatis, *Phys. Rev. B* **55**, 7464 (1997).
- [48] S. Zhang, J. Carlson, and J. E. Gubernatis, *Phys. Rev. Lett.* **74**, 3652 (1995).
- [49] J. Wang, X. Zhang, R. Ma, G. Yang, E. V. Castro, and T. Ma, *Phys. Rev. B* **106**, 134513 (2022).
- [50] J. E. Hirsch and H. Q. Lin, *Phys. Rev. B* **37**, 5070 (1988).
- [51] H. Q. Lin, J. E. Hirsch, and D. J. Scalapino, *Phys. Rev. B* **37**, 7359 (1988).